



Laterally configured resistive switching device based on transition-metal nano-gap electrode on Gd oxide

Masatoshi Kawakita, Kyota Okabe, and Takashi Kimura

Citation: *Applied Physics Letters* **108**, 023101 (2016); doi: 10.1063/1.4939683

View online: <http://dx.doi.org/10.1063/1.4939683>

View Table of Contents: <http://scitation.aip.org/content/aip/journal/apl/108/2?ver=pdfcov>

Published by the *AIP Publishing*

Articles you may be interested in

[Role of metal-oxide interfaces in the multiple resistance switching regimes of Pt/HfO₂/TiN devices](#)

Appl. Phys. Lett. **107**, 023504 (2015); 10.1063/1.4926340

[Effects of electrode material and configuration on the characteristics of planar resistive switching devices](#)

APL Mater. **1**, 052106 (2013); 10.1063/1.4827597

[Low voltage resistive switching devices based on chemically produced silicon oxide](#)

Appl. Phys. Lett. **103**, 062104 (2013); 10.1063/1.4817970

[Effect of conductive atomic force microscope tip loading force on tip-sample interface electronic characteristics: Unipolar to bipolar resistive switching transition](#)

Appl. Phys. Lett. **103**, 051604 (2013); 10.1063/1.4817380

[Field-induced resistive switching in metal-oxide interfaces](#)

Appl. Phys. Lett. **85**, 317 (2004); 10.1063/1.1768305

The image shows the cover of an Applied Physics Reviews journal issue. It features a blue and orange color scheme with a molecular structure background. The text 'NEW Special Topic Sections' is prominently displayed in white. Below it, the text 'NOW ONLINE' is in yellow, followed by 'Lithium Niobate Properties and Applications: Reviews of Emerging Trends' in white. The AIP Applied Physics Reviews logo is in the bottom right corner.

NEW Special Topic Sections

NOW ONLINE
Lithium Niobate Properties and Applications:
Reviews of Emerging Trends

AIP Applied Physics
Reviews

Laterally configured resistive switching device based on transition-metal nano-gap electrode on Gd oxide

Masatoshi Kawakita,¹ Kyota Okabe,¹ and Takashi Kimura^{1,2,a)}

¹Department of Physics, Kyushu University, 6-10-1 Hakozaki, Fukuoka 812-8581, Japan

²Research Center for Quantum Nano-Spin Sciences, Kyushu University, 6-10-1 Hakozaki, Fukuoka 812-8581, Japan

(Received 13 October 2015; accepted 26 December 2015; published online 11 January 2016)

We have developed a fabrication process for a laterally configured resistive switching device based on a Gd oxide. A nano-gap electrode connected by a Gd oxide with the ideal interfaces has been created by adapting the electro-migration method in a metal/GdO_x bilayer system. Bipolar set and reset operations have been clearly observed in the Pt/GdO_x system similarly in the vertical device based on GdO_x. Interestingly, we were able to observe a clear bipolar switching also in a ferromagnetic CoFeB nano-gap electrode with better stability compared to the Pt/GdO_x device. The superior performance of the CoFeB/GdO_x device implies the importance of the spin on the resistive switching. © 2016 AIP Publishing LLC. [<http://dx.doi.org/10.1063/1.4939683>]

Resistive switching device consisting of a metallic oxide layer sandwiched by the metallic electrodes has paid considerable attention as a next-generation nonvolatile memories owing to its simple device structure with low power consumption.^{1–3} Moreover, the nonlinear transport property with memorizing the applied voltage history is expected to contribute the development of the innovative logic circuits such as neuromorphic and learning-type devices.^{4–9} As the origins for the transition between the low-resistive and high-resistive states, two major mechanisms—filament-type and interface-type models—are proposed.¹ However, the microscopic mechanism for the resistance change is still a controversial issue under the irreconcilable conflicts between the above two models, and the dominant mechanism seems to depend on the preparation condition of the devices. Since the establishment of the device fabrication with the operation under the mechanism control is an important milestone for the reliable and low-power-consumption operations, proper understanding of the mechanism of the resistance change is a key for the development of the resistive switching device. In addition, the development of more simple and flexible fabrication processes is also important from the view point of the cost-competitive device compared to the conventional flash memory based on the floating-gate transistor.

Apart from the device fabrication, it should be noted that most of the metallic oxides showing the resistive switching include the transition metals with finite magnetic moments.^{10–18} This implies that the resistance switching is related to the spin configuration in the metallic oxide. Especially, the interface between magnetic metal and magnetic oxide show various functional properties through the exchange interaction.¹⁹ Moreover, the resistive switching devices with the ferromagnetic electrode have been reported in the vertical stack structures although the switching mechanisms do not seem to be related to the spin.^{20,21} If one can demonstrate the resistive switching operation with additional spin functionalities, we may have greater control based on

the direction of the spin in the magnetic oxide. A laterally configured structure is suitable for demonstrating such attractive properties because of high flexibility of the device geometry. However, most of the resistive switching devices reported so far consist of vertical stack structures because of the regulation of the short channel length in the metallic oxide. This is because the operation voltage is believed to be proportional to the channel length of the oxide layer. Moreover, the difficulty for the preparation of the clean metal/oxide interface without using vertical stack structures is another important reason. From these view points, in the present study, we developed an original method for the fabrication of the resistive switching device in lateral configuration and investigated the influence of the ferromagnetic electrode and spin orientation on the switching property.

To fabricate laterally configured switching devices with ideal clean interfaces, we used a break junction technique,^{22–24} whose process is schematically shown in Fig. 1(a). First, we prepared a patterned metal/oxide bilayer with a nanoconstruction on a SiO₂/Si substrate. In the present study, we adapted GdO_x to a metallic oxide layer. For the metallic layer, we used Pt and CoFeB. Here, the metal/oxide bilayer film have been continuously deposited on the resist template patterned by electron beam lithography by the magnetron sputtering under the base pressure of 10^{–6} Pa. Gd oxide (GdO_x) has been grown by the magnetron reactive sputtering of the Gd in a mixed gas of Ar and O₂ with the O₂ flow ratio of 1/7. The chemical composition for GdO_x is unclear, but its electrical property is highly insulating. To prevent the distribution of the composition, we made all of the devices reported here almost same time. Here, the thicknesses for Gd oxide and metallic electrodes are 100 nm and 30 nm, respectively. The electrical resistivities for Pt and CoFeB are, respectively, 32 μΩ cm and 52 μΩ cm. Figure 1(c) shows a scanning electron microscope (SEM) image of the fabricated electrode pattern consisting of the Pt/GdO_x bilayer after the lift-off process. A nano-gap electrode was formed by using an electro-migration technique with the real-time monitoring of the current. In the bilayer system, the current almost perfectly

^{a)}t-kimu@phys.kyushu-u.ac.jp

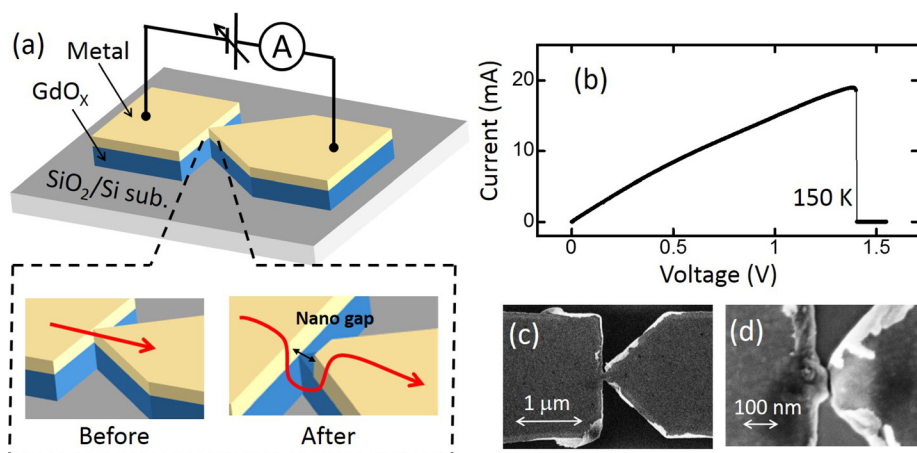


FIG. 1. (a) Schematic illustrations of a laterally configured resistive switching device and formation process of nano-gap electrode. (b) I - V characteristic measurement during nano-gap formation process SEM images. (c) before the nano-gap formation and (d) after the nano-gap formation.

flows in the metallic layer because of the large difference of the electrical resistivity. The wire pattern was an asymmetric structure formed by the connection between triangular and rectangular electrodes. Since the current density becomes maximum at the boundary between the triangular and rectangular electrode in this structure, the nano-gap will be formed around the boundary. We performed a break-junction experiment at low temperature in order to further increase the electrical insulation of the oxide layer and to minimize the gap length. As shown in Fig. 1(b), the nanogap formation was clearly distinguished by monitoring the flowing current. Figure 1(d) shows a SEM image of the typically fabricated nano-gap electrode. A nanogap whose gap length is less than 10 nm has been obtained. Finally, we were able to fabricate a laterally configured metallic/oxide/metallic junction with the clean interfaces as schematically shown in Fig. 1(a). After the nano-gap formation, the resistance switching properties were evaluated by measuring the I - V characteristic. To clarify the correlation between the interface condition and device performance, we also fabricated the similar planar device with non-ideal interface, where the metal/oxide interface has been formed by *ex-situ* sputtering process with breaking the vacuum.

First, we evaluated the lateral Pt/GdO_x device, which is a typical material combination in the vertical devices based on Gd-oxide.²⁵ We measured I - V characteristics after the formation of the nanogap. Figure 2(a) shows a representative result of the I - V characteristic observed in the laterally configured Pt/GdO_x switching device. Clear resistance switchings with set and reset transitions were observed. Here, the resistance for the low resistive state R_{LRS} and that for the high resistive state R_{HRS} were approximately 3 kΩ and 50 kΩ, corresponding to 1500% resistance change, which is defined by $(R_{HRS} - R_{LRS})/R_{LRS}$. This value was slightly smaller than those reported in the vertical device with the superior performance.^{25,26} We believe that this is because the resistance of the metallic electrode was much higher than the vertical situation. Since R_{LRS} can be reduced by increasing the width of thickness for the patterned electrode, a resistance change in the lateral device can be comparable to the vertical devices. Interestingly, the switching voltages for set and reset transitions were, respectively, 1.1 V and -1.2 V, which were relatively low compared to those in the vertical devices. Since the low voltage operation leads to the

reduction of the power consumption,²⁶ this is the strong advantage of the laterally configure device. We also emphasize that the transition curve shown in Fig. 2(a) has been obtained from the virgin curve without performing the filament forming process.²⁷ Although the voltage of 1.5 V, which is slightly higher than that in the I - V measurements,

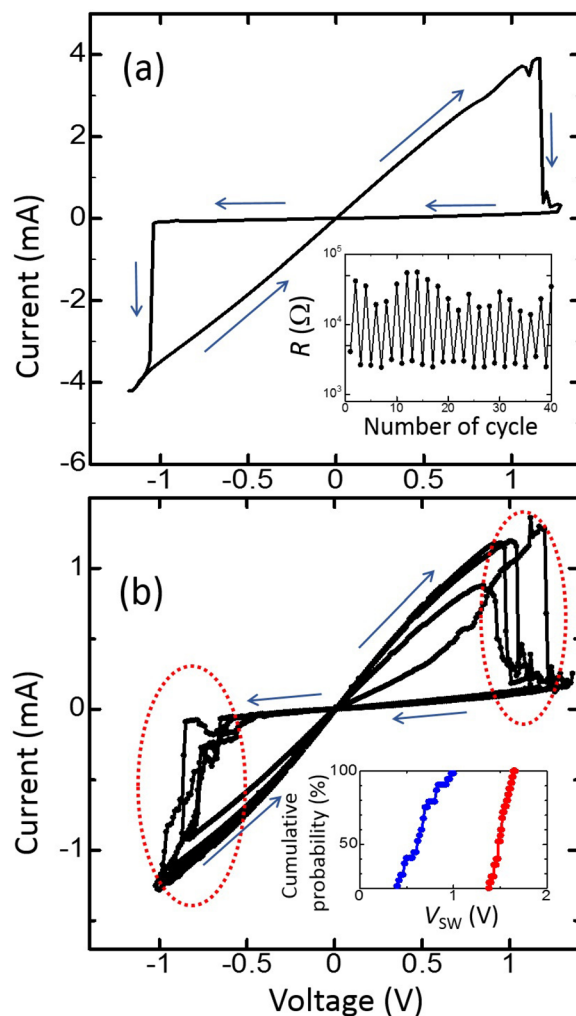


FIG. 2. (a) Representative I - V characteristic for a lateral Pt/GdO_x device exhibiting clear set and reset processes. The inset shows the switching endurance property of the fabricated device. (b) Dispersion of I - V characteristics for the lateral Pt/GdO_x device with the intermediate resistance state. The inset shows the distribution of the switching voltages for set and reset processes.

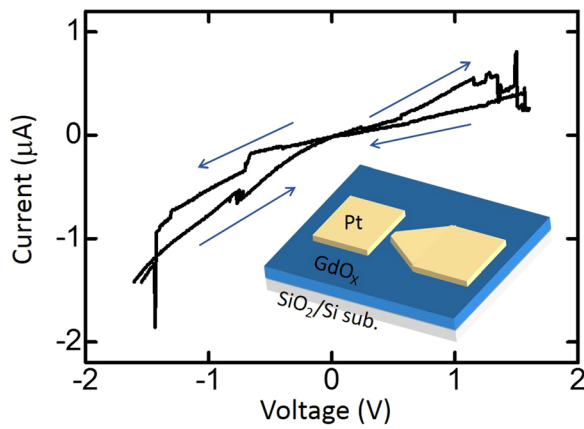


FIG. 3. I - V characteristic for a Pt-nano-gap device fabricated on GdO_x film with unstable transport property.

had been applied during the nano-gap forming process, it had been performed at low temperature. Therefore, we expected that the nano-gap forming process could not play an important role for the filament forming process. Moreover, we did not observe unipolar-type switching in the voltage range from -4 V to 4 V.²⁸ In addition, the I - V curve at a high resistance state is well reproduced by a Schottky characteristics. These facts imply that the main mechanism of the resistance switching is interface type.

We also demonstrated a high endurance of the switching property from the application of the alternative voltage as shown in the inset of Fig. 2(a). Thus, the validity of the fabrication technique for the resistive switching device with a lateral configuration has been confirmed. We found that 70% devices among 20 devices showed clear bipolar switching. Although the device dependence of the switching voltages was small, the resistance at low resistive state strongly depends on sample to sample. This is probably because the effective junction size for the switching shows the strong sample dependence. The control of the junction size is an important milestone for this fabrication method. Moreover, we often observed intermediate resistive states under the high bias condition just after the transition as shown in Fig. 2(b) in some of the devices. In addition, the switching voltage for set and reset processes showed large dispersions, as shown in the inset of Fig. 2(b). At the moment, the detailed mechanism of the switching and the intermediate state are still unclear but may be related to the interface condition.²⁹

To clarify the influence of the interface condition on the switching more clearly, we also evaluated the resistive switching property of the Pt/ GdO_x sample with the non-ideal interfaces. As schematically shown in the inset of Fig. 3, the patterned asymmetric Pt electrode has been fabricated on a uniform GdO_x film by using a conventional lift-off technique. Here, we did not perform any interface treatment such as Ar ion milling and wet-etching processes. Therefore, the residual resist, other organic components and/or natural oxidation layer may exist at interface between Pt and GdO_x .³⁰ Figure 3 shows the I - V characteristics after the nano-gap formation. Although the switching behaviors have been observed, the resistance change due to the transition is quite small. Especially, in lower resistance state, the resistance

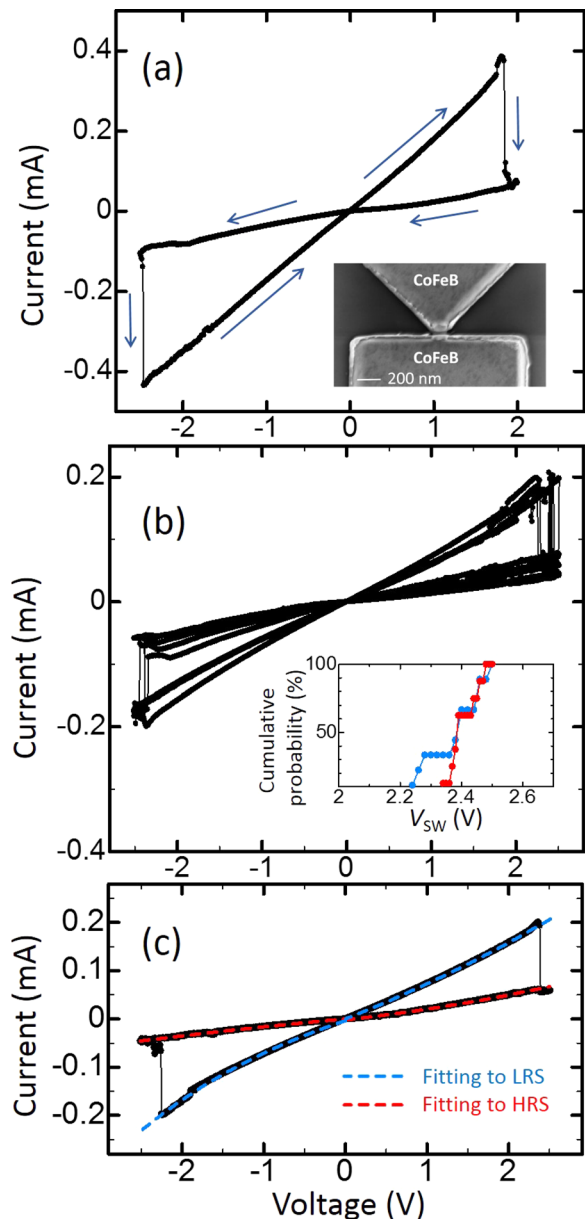


FIG. 4. (a) Representative I - V characteristic for a lateral CoFeB/ GdO_x device together with the SEM image in the vicinity of the junction. (b) Dispersion of I - V characteristic for the lateral CoFeB/ GdO_x device with the intermediate resistance state. The inset shows the distribution of the switching voltages for set and reset processes. (c) Representative HRS and LRS I - V curves fitted to the equations for the Schottky barrier.

value was much higher than that in the previous device. This is probably due to the non-clean condition for the interface between Pt and GdO_x . Thus, the interface condition was confirmed to play an important role for obtaining the effective resistance switching.

We then investigate the material dependence of metallic electrode on the switching property. We fabricate the resistive switching device using ferromagnetic CoFeB electrode. Here, because of its large resistivity and low heat conductivity for CoFeB electrode, it was difficult to obtain the nano-gap less than 10 nm. The size of the nanogap is approximately 20 nm, but it is difficult to estimate precise electrode distance only from the SEM image. As discussed earlier, the direct connection between CoFeB and GdO_x

induces the exchange interaction at the interface.¹⁹ In addition, the electric current from the ferromagnetic electrode generates the spin-polarized current, which exerts the torque in the magnetic moment via spin transfer torque.³¹ These additional effects originating from the ferromagnetic metal may affect the switching property, leading to the additional controllability utilizing the spins. Figure 4(a) shows the I - V characteristics after the formation of CoFeB nanogap. Interestingly, we clearly observed bipolar switching behavior also in CoFeB/GdO_x device at room temperature. We quantitatively evaluated the I - V characteristics in CoFeB/GdO_x devices. The resistance change due to the switching was smaller than that in the Pt/GdO_x device. This is mainly because the transport at the high resistive state is more conductive than that in the Pt/GdO_x device. The switching voltages both for set and reset transitions were also higher than those in the Pt/GdO_x device. Thus, the device performance for CoFeB/GdO_x device seems to be worthy than that for the Pt/GdO_x device. However, there are several advantages in CoFeB/GdO_x devices compared to the Pt/GdO_x device, as follows. Figure 4(b) shows the distribution of the I - V curves in another CoFeB device. Although a variation of R_{HRS} seems to be not so small, the distribution of the switching voltage is quite small compared to the Pt/GdO_x device, as shown in the inset of Fig. 4(b). Moreover, in the CoFeB-based devices, we have never observed the intermediate state between the high and low resistance observed in Fig. 2(c). In addition, it should be noted that the I - V curves both for the low and high resistive states are well reproduced by the Schottky characteristics, as shown in Fig. 4(c), strongly suggesting the interface-type switching.³² Since our CoFeB film was confirmed to have an efficient spin polarization and saturation magnetization, these superior stabilities obtained in CoFeB-based devices may be related to the spin-polarized CoFeB electrodes and/or the exchange interaction play an important role for the resistance switching. However, it should be noted that the switching endurance for the CoFeB-based device is worse than that for Pt-based device. This may be related to the higher switching voltage in CoFeB electrode with the Schottky interface and relatively wide nanogap electrode.

In short, by performing the electro-migration technique in a transition metal/Gd oxide bilayer, we have fabricated a nano-gap electrode on a Gd oxide. The I - V characteristics for the nano-gap electrode showed bipolar switching behaviors, which are consistent with the results in the vertical resistive switching device based on Gd oxide. We have also investigated the influence of the ferromagnetic electrode on the resistive switching and observed more stable bipolar switching property than that in the Pt/GdO_x system. The results imply that the spins both in metal and oxide play an important role in the resistive switching process.

This work was partially supported by Grant-in-Aid for Scientific Research on Innovative Area, “Nano Spin Conversion Science” (26103002) and that for Scientific Research (S)(25220605).

- ¹A. Sawa, *Mater. Today* **11**, 28 (2008).
- ²R. Waser and M. Aono, *Nat. Mater.* **6**, 833 (2007).
- ³F. Pan, S. Gao, C. Chen, C. Song, and F. Zeng, *Mater. Sci. Eng. R* **83**, 1 (2014).
- ⁴G. Indiveri, B. Linares-Barranco, R. Legenstein, G. Deligeorgis, and T. Prodromakis, *Nanotechnology* **24**, 384010 (2013).
- ⁵S. H. Jo, T. Chang, I. Ebong, B. B. Bhadviya, P. Mazumder, and W. Lu, *Nano Lett.* **10**, 1297 (2010).
- ⁶S. Yu, Y. Wu, R. Jeyasingh, D. Kuzum, and H.-S. P. Wong, *IEEE Trans. Electron Devices* **58**, 2729 (2011).
- ⁷D. B. Strukov and H. Kohlstedt, *MRS Bull.* **37**, 108 (2012).
- ⁸D. B. Strukov, G. S. Snider, D. R. Stewart, and R. S. Williams, *Nature* **453**, 80 (2008).
- ⁹T. Hasegawa, T. Ohno, K. Terabe, T. Tsuruoka, T. Nakayama, J. K. Gimzewski, and M. Aono, *Adv. Mater.* **22**, 1831 (2010).
- ¹⁰S. Q. Liu, N. J. Wu, and A. Ignatiev, *Appl. Phys. Lett.* **76**, 2749 (2000).
- ¹¹X. Cao, X. Li, X. Gao, W. Yu, X. Liu, Y. Zhang, L. Chen, and X. Cheng, *J. Appl. Phys.* **106**, 073723 (2009).
- ¹²Z. Yan, Y. Guo, G. Zhang, and J.-M. Liu, *Adv. Mater.* **23**, 1351 (2011).
- ¹³K. A. Bogle, M. N. Bachhav, M. S. Deo, N. Valanoor, and S. B. Ogale, *Appl. Phys. Lett.* **95**, 203502 (2009).
- ¹⁴G. Chen, C. Song, C. Chen, S. Gao, F. Zeng, and F. Pan, *Adv. Mater.* **24**, 3515 (2012).
- ¹⁵K. Nagashima, T. Yanagida, K. Oka, M. Taniguchi, T. Kawai, J.-S. Kim, and B. H. Park, *Nano Lett.* **10**, 1359 (2010).
- ¹⁶S. Muraoka, K. Osano, Y. Kanzawa, S. Mitani, S. Fujii, K. Katayama, Y. Katoh, Z. Wei, T. Mikawa, K. Arita, Y. Kawashima, R. Azuma, K. Kawai, K. Shimakawa, A. Odagawa, and T. Takagi, *IEDM Tech. Dig.* **2007**, 779.
- ¹⁷I. Hwang, M.-J. Lee, G.-H. Buh, J. Bae, J. Choi, J.-S. Kim, S. Hong, Y. S. Kim, I.-S. Byun, S.-W. Lee, S.-E. Ahn, B. S. Kang, S.-O. Kang, and B. H. Park, *Appl. Phys. Lett.* **97**, 052106 (2010).
- ¹⁸C. Yoshida, K. Kinoshita, T. Yamasaki, and Y. Sugiyama, *Appl. Phys. Lett.* **93**, 042106 (2008).
- ¹⁹S. Chikazumi, *Physics of Magnetism* (Wiley, New York, 1964).
- ²⁰L. W. Feng, C. Y. Chang, Y. F. Chang, W. R. Chen, S. Y. Wang, and P. W. Chiang, *Appl. Phys. Lett.* **96**(5), 052111 (2010).
- ²¹L. W. Feng, C. Y. Chang, Y. F. Chang, T. C. Chang, S. Y. Wang, S. C. Chen, C. C. Lin, S. C. Chen, and P. W. Chiang, *Appl. Phys. Lett.* **96**, 222108 (2010).
- ²²T. Taychatanapat, K. I. Bolotin, F. Kuemmeth, and D. C. Ralph, *Nano Lett.* **7**, 652 (2007).
- ²³H. Park, A. K. L. Lim, A. P. Alivisatos, J. Park, and P. L. McEuen, *Appl. Phys. Lett.* **75**, 301 (1999).
- ²⁴A. K. Mahapatro, S. Ghosh, and D. B. Janes, *IEEE Trans. Nanotechnol.* **5**, 232 (2006).
- ²⁵J.-C. Wang, Y.-R. Ye, J.-S. Syu, P.-R. Wu, C.-I. Wu, P.-S. Wang, and J. H. Chang, *Jpn. J. Appl. Phys., Part 1* **52**, 04CD07 (2013).
- ²⁶D. Jana, S. Maikap, T. C. Tien, H. Y. Lee, W.-S. Chen, F. T. Chen, M.-J. Kao, and M.-J. Tsai, *Jpn. J. Appl. Phys., Part 1* **51**, 04DD17 (2012).
- ²⁷A. Prakash, S. Maikap, W. Banerjee, D. Jana, and C.-S. Lai, *Nanoscale Res. Lett.* **8**, 379 (2013).
- ²⁸T. Miyabe and T. Nakaoka, *Jpn. J. Appl. Phys., Part 1* **52**, 04CJ08 (2013).
- ²⁹C.-Y. Lin, C.-Y. Wu, C.-Y. Wu, T.-Y. Tseng, and C. Hu, *J. Appl. Phys.* **102**, 094101 (2007).
- ³⁰A. N. Broers, W. W. Molzen, J. J. Cuomo, and N. D. Wittels, *Appl. Phys. Lett.* **29**, 596 (1976).
- ³¹D. C. Ralph and M. D. Stiles, *J. Magn. Magn. Mater.* **320**, 1190 (2008).
- ³²A. Sawa, T. Fujii, M. Kawasaki, and Y. Tokura, *Jpn. J. Appl. Phys., Part 1* **44**, L1241 (2005).